Pan1 regulates transitions between stages of clathrin-mediated endocytosis

Mary Katherine Bradford, Karen Whitworth, and Beverly Wendland
Department of Biology, Johns Hopkins University, Baltimore, MD 21218

ABSTRACT **Endocytosis is a well-conserved process by which cells invaginate small portions of the plasma membrane to create vesicles containing extracellular and transmembrane cargo proteins. Dozens of proteins and hundreds of specific binding interactions are needed to coordinate and regulate these events. *Saccharomyces cerevisiae* is a powerful model system with which to study clathrin-mediated endocytosis (CME). Pan1 is believed to be a scaffolding protein due to its interactions with numerous proteins that act throughout the endocytic process. Previous research characterized many Pan1 binding interactions, but due to Pan1's essential nature, the exact mechanisms of Pan1's function in endocytosis have been difficult to define. We created a novel Pan1-degron allele, Pan1-AID, in which Pan1 can be specifically and efficiently degraded in <1 h upon addition of the plant hormone auxin. The loss of Pan1 caused a delay in endocytic progression and weakened connections between the coat/actin machinery and the membrane, leading to arrest in CME. In addition, we determined a critical role for the central region of Pan1 in endocytosis and viability. The regions important for endocytosis and viability can be separated, suggesting that Pan1 may have a distinct role in the cell that is essential for viability.**

Monitoring Editor
Sandra L. Schmid
University of Texas
Southwestern Medical Center

Received: Nov 10, 2014
Revised: Jan 13, 2015
Accepted: Jan 23, 2015

INTRODUCTION

Clathrin-mediated endocytosis (CME) is the critical process by which portions of the plasma membrane and associated cargoes are delivered to the cell interior. The process supports membrane homeostasis, signal transduction, drug delivery, and nutrient uptake. More than 50 different proteins are involved in the initiation, maturation, and scission of events at endocytic sites, or patches, and most of these proteins and their functions are well conserved between yeast and mammals. Formation of the clathrin coat, which consists of clathrin, adaptor proteins, early/late coat proteins, and actin-regulatory complexes, begins with the recruitment of early coat and adaptor proteins to the plasma membrane. The adaptors bind to cargo, late coat proteins, and clathrin and connect the newly forming coat to the plasma membrane. Additional coat components associate at the endocytic patch and recruit proteins for the final stages of endocytosis. Actin and actin-regulatory proteins are recruited to the patch to invaginate the membrane and form the vesicle. Finally, scission proteins complete the process by pinching off the newly formed vesicle from the plasma membrane, allowing the vesicle to be propelled into the cell through the force produced by actin polymerization. Through phosphorylation and dephosphorylation of both proteins and lipids, the clathrin coat dissociates from the vesicle, and proteins are recycled through the cytosol and back to the membrane to participate in further rounds of CME.

The yeast protein Pan1 is best known as a CME coat protein that can interact with adaptors, early and late coat proteins, and actin-regulatory proteins; thus Pan1 is presumed to act as a central scaffold that links the early and late stages of endocytosis (Sachs and Deardorff, 1992; Wendland *et al.*, 1996). Pan1 is a homologue of the mammalian protein Intersectin, which is also believed to be a CME scaffold (Yamabhai *et al.*, 1998; Hussain *et al.*, 1999). Pan1 is 1480 residues long and contains two N-terminal Eps15-homology (EH) domains, a central, largely disordered region containing several predicted short coiled-coils, and a C-terminal actin regulatory domain. The N-terminus is composed of two long repeat regions (LR1 and LR2) that each contain an EH domain. The two EH domains are 72% similar, yet only the second domain can bind to EH ligands (Asn-Pro-Phe tripeptide motifs of the endocytic adaptor proteins Ent1/2 and

This article was published online ahead of print in MBoC in Press (http://www.molbiolcell.org/cgi/doi/10.1091/mbc.E14-11-1510) on January 28, 2015.

Address correspondence to: Beverly Wendland (bwendland@jhu.edu).

Abbreviations used: AID, auxin-inducible degron; CME, clathrin-mediated endocytosis; EH, Eps15 homology; EV, empty vector; IAA, indoleacetic acid; LR, long repeat; WT, wild type.

Yap1801/2; Salcini *et al.*, 1997; Paoluzi *et al.*, 1998; Wendland and Emr, 1998; Wendland *et al.*, 1999; Maldonado-Baez *et al.*, 2008). Pan1 forms a complex with Sla1 and End3, which bind its N-terminus and central region, respectively (Tang *et al.*, 1997, 2000; Whitworth *et al.*, 2014). Through its central region, Pan1 can form homodimers and homo-oligomers and binds the coat protein Sla2 (Miliaras and Wendland, 2004; Toshima *et al.*, 2005, 2007; Pierce *et al.*, 2013). The central region also contains three proposed nuclear localization signals (NLSs; Kamińska *et al.*, 2007). Pan1 regulates actin polymerization through motifs in its C-terminal region, which bind Arp2/3, F-actin, and the type I myosins Myo3/5 (Duncan *et al.*, 2001; Toshima *et al.*, 2005; Barker *et al.*, 2007). The C-terminus has also been implicated in binding to the coiled-coil region of the early coat protein Ede1 (S. Barker and B. Wendland, unpublished observations). Pan1 is heavily phosphorylated by the evolutionarily conserved protein kinases Ark1/Prk1, which is believed to negatively regulate Pan1's interactions with other coat proteins to promote dissociation of the vesicular coat (Tang *et al.*, 2000; Zeng *et al.*, 2001; Toshima *et al.*, 2005, 2007). To allow reuse, Pan1 is dephosphorylated by Glc7 (Zeng *et al.*, 2007). Due to Pan1's numerous interactions throughout the endocytic process, it is well suited to be a key coordinator for maturation of the endocytic coat from early to late stages.

Deletion of a gene encoding a late coat protein leads to increased patch lifetimes of the remaining coat proteins, indicating an arrest or a stall in the pathway (Kaksonen *et al.*, 2005). In these same cells, actin polymerization is often increased or unregulated at the patch (Kaksonen *et al.*, 2003, 2005; Skruzny *et al.*, 2012). Pan1's essential nature makes deletion experiments impossible. Work with *pan1* mutant alleles suggests roles for Pan1 in endocytosis, actin cytoskeletal organization, polarized cell growth, and mitochondrial protein sorting (Zoladek *et al.*, 1995; Tang and Cai, 1996; Wendland *et al.*, 1996; Bidlingmaier *et al.*, 2001; Kamińska *et al.*, 2005). However, its precise mechanistic role(s) in these pathways is unknown, nor is it known which of these, if any, corresponds to Pan1's essential function(s). Pan1 binds early and late endocytic factors, and thus we hypothesized that its deletion would cause misregulation of recruitment of endocytic proteins to and lifetimes at the patch. In addition, although Pan1 is itself not a strong regulator of actin polymerization, it does bind several proteins involved in actin polymerization (both promotion and inhibition); therefore it is predicted that Pan1 deletion could cause aberrant actin structure formation (Duncan *et al.*, 2001; Toshima *et al.*, 2005; Barker *et al.*, 2007). Recent work with Pan1 containing mutated or deleted EH domains found that Pan1's EH domains are not critical for patch formation or efficient endocytosis but may be important for the patch lifetime regulation of some coat proteins. The mild phenotype of these mutant alleles is most likely due to the redundancy of EH domains in End3 and Ede1, which are also found at endocytic patches (Suzuki *et al.*, 2012).

Much of the previous work on Pan1 has been done using temperature-sensitive (*ts*) conditional mutants; however, findings using *ts* alleles are confounded by the effects of the nonpermissive conditions, which can adversely affect endocytosis and elicit a stress response. Further, these allele experiments are chronic and could be subject to compensatory changes. Finally, it is not known whether these alleles remove some or all Pan1 functions. Conditional expression of Pan1 has been unsuccessful due to putative alternative translational start sites and "leaky" expression of truncated protein even in the nonpermissive conditions (Tang and Cai, 1996; K. Whitworth and B. Wendland, unpublished results). Thus it was necessary to create a degron allele of Pan1 that acutely and specifically degrades Pan1 protein in vivo. Using the auxin-inducible degron (AID; Nishimura *et al.*, 2009), Pan1 was degraded in <1 h and, for the first time, acute endocytic phenotypes in the absence of Pan1 were observed.

Using Pan1-AID, we characterized the effects of Pan1 loss on CME and determined which regions of Pan1 are critical for its functions in viability and endocytosis. In Pan1-AID, CME is quickly arrested, and the progression between the early and late coat stages is delayed in the absence of the scaffolding function of Pan1. At the few patches that did form, actin polymerization was aberrant, leading to the formation of dynamic actin flares containing coat components but no invaginating membrane, suggesting a role for Pan1 in actin regulation and the coordination of coat interactions. We identified a region of Pan1 spanning the second EH domain and central region that was critical for viability and endocytosis. In addition, we defined regions of Pan1 that supported viability and not endocytosis, suggesting that Pan1 may have an additional role(s) independent of endocytosis.

RESULTS

Efficient and specific depletion of Pan1 protein using Pan1-AID

To investigate the function(s) of Pan1, we used the AID system to acutely deplete cells of Pan1 protein in vivo (Nishimura *et al.*, 2009). The Pan1-AID degron cells were created by endogenously C-terminally tagging Pan1 with the AID sequence and integrating the *OsTIR1* gene with the constitutive ADH1 promoter. OsTIR1 is a plant F-box protein that specifically binds and promotes the degradation of the AID-tagged target protein only in the presence of auxin. For controls, we used a wild-type (WT) strain and a strain containing only OsTIR1 (TIR1) with empty vector (EV) plasmids; these strains grew similarly in the absence and presence of auxin (Figure 1A). In the absence of auxin, Pan1-AID cells grew to WT levels, and Pan1 protein was stable; upon addition of auxin, growth was arrested, and 84% of Pan1 protein was degraded within 15 min (Figure 1, A and B). Depletion of Pan1 was specific and did not affect the stability of its binding partners Sla1 and End3; however, there was a gel mobility shift for Sla1 upon the addition of auxin (Figure 1C). This gel mobility shift of Sla1 was not seen in extracts from TIR1 cells treated with auxin, suggesting that the shift was due to the loss of Pan1, consistent with a predicted hyperphosphorylation phenotype (Figure 1, C and D; Zeng *et al.*, 2001, 2007). It has been proposed that auxin (specifically, indoleacetic acid [IAA]) can induce filamentous growth, adhesion, and/or growth arrest in WT cells; however, we did not observe any of these phenotypes in our experiments (Prusty *et al.*, 2004).

To determine whether the degradation of Pan1 led to either growth arrest or cell death, we grew cells in the absence or presence of auxin and stained dead cells with propidium iodide and quantified them by flow cytometry. After 24 h in the presence of auxin, Pan1-AID cells with EV reached almost 100% death, whereas death of the control strains was at similar levels to those with no auxin present (Figure 1E). To relate cell death to reduced Pan1 protein levels, we analyzed cell death over time. We found that Pan1-AID cells reach ~50% death after 4 h in the presence of auxin, with >75% of cells still alive between 0 and 2 h (Figure 1F). These early time points were used to assess the acute phenotypes of Pan1 depletion on living cells. The Pan1-AID growth (Figure 1A) and death (Figure 1, E and F) phenotypes were restored to WT levels with expression of full-length Pan1 from a plasmid.

Together these experiments show that Pan1-AID is a robust, efficient system for investigating the acute effects of Pan1 depletion in vivo.

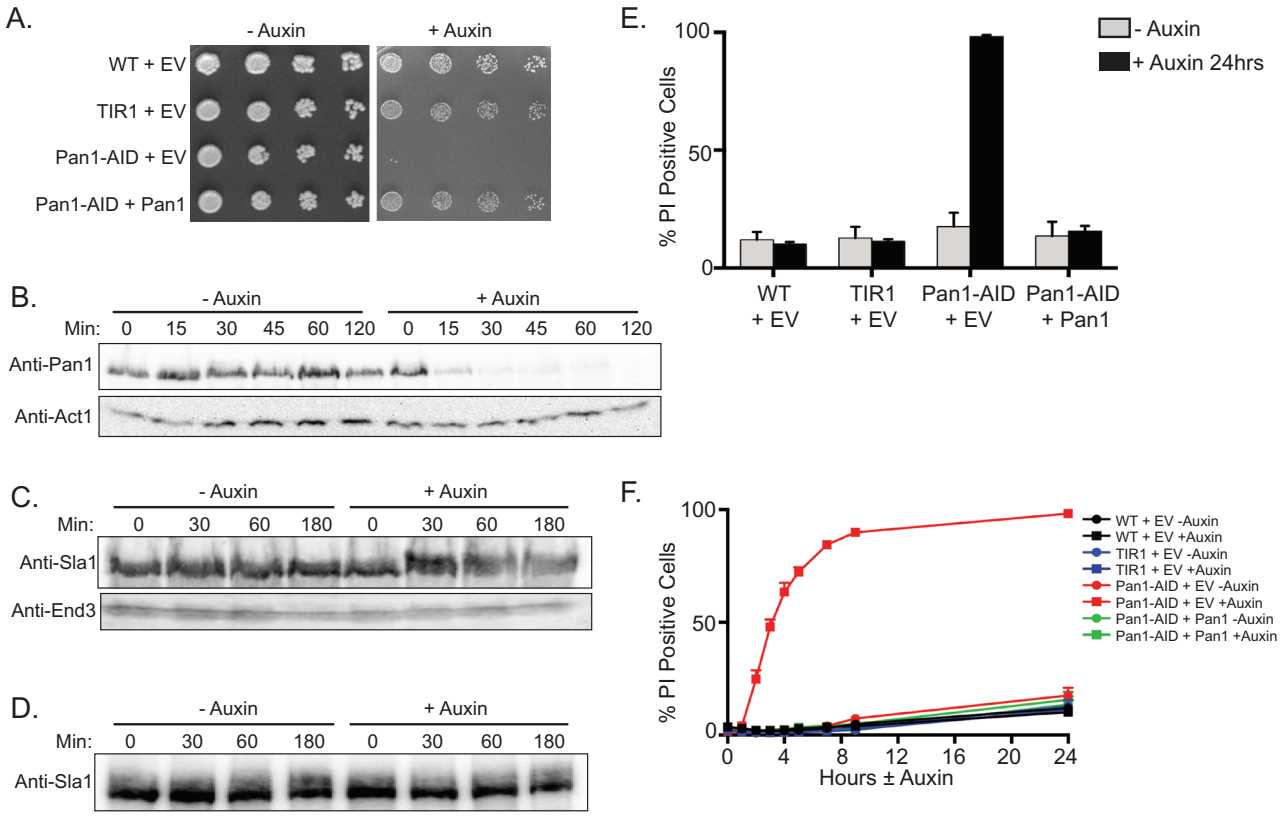

FIGURE 1: Pan1-AID is an efficient tool for depleting Pan1 protein in cells. (A) Serial dilutions of cells of indicated genotype were grown on synthetic medium ± auxin for 3 d at 30°C. Immunoblots detecting Pan1, Sla1, and End3 in Pan1-AID (B, C) or TIR1 (D) cell lysates grown for indicated time ± auxin. Act1 serves as a loading control in B. (E) Percentage of cells that were positively stained with propidium iodide (PI) after growth for 24 h ± auxin at 30°C was quantified by flow cytometry. Average of three replicate experiments (mean ± SD). (F) Strains were grown ± auxin and samples collected at indicated times, stained with PI, and quantified by flow cytometry. Average of three replicate experiments (mean ± SD).

Endocytosis is arrested upon acute depletion of Pan1

Pan1's best-characterized role in the cell is as an endocytic coat protein. Previous studies showed that endocytosis is aberrant in *pan1* mutant cells; thus we hypothesized that endocytosis would be significantly affected in Pan1-AID cells upon depletion of Pan1 by the addition of auxin. We monitored bulk endocytosis using the lipophilic dye FM4-64 (Figure 2A). Cells were incubated in the absence and presence of auxin for 30 min and then stained with FM4-64 in similar auxin conditions for 15 min. In the control strains, WT and TIR1 plus EV, in the absence and presence of auxin and in Pan1-AID cells in the absence of auxin, the cells efficiently internalized the dye, which was trafficked throughout the cell, highlighting internal structures such as endosomes and vacuoles. In contrast, FM4-64 was trapped at the plasma membrane in the Pan1-AID with EV cells plus auxin, indicating that bulk endocytosis had been arrested upon depletion of Pan1. This endocytic arrest was rescued by expressing full-length Pan1 from a plasmid.

To observe receptor-mediated CME, we used chimeras of the methionine permease Mup1 with pHluorin (pHl), a pH-sensitive variant of green fluorescent protein (GFP; Miesenböck *et al.*, 1998). In the absence of methionine in the growth medium, Mup1 is localized to the plasma membrane; upon addition of methionine, Mup1 is quickly endocytosed through CME and targeted to the vacuole lumen. The pHluorin signal is quenched in the acidic lumen of the late endosome/multivesicular bodies (MVBs) and vacuoles. Thus endocytic efficiency can be quantified by measuring the amount of fluorescence remaining after the addition of methionine (Prosser *et al.*, 2010). In the absence of auxin, WT, TIR1, and Pan1-AID cells internalized Mup1-pHl to similar levels after the addition of methionine (Figure 2, B and C). The addition of auxin did not affect Mup1-pHl internalization for the control cells. However, when Pan1-AID cells were pretreated with auxin for 30 min before addition of methionine, Mup1 remained at the plasma membrane, again confirming that the absence of Pan1 causes an endocytic arrest. This arrest in endocytosis was fully rescued by expressing full-length Pan1 from a plasmid in the Pan1-AID cells.

In the absence of both auxin and methionine, all strains exhibited brighter fluorescence at the plasma membrane over the time course. We hypothesize this is due to the continued production of Mup1-pHl that is trafficked to the plasma membrane. The addition of auxin alone appears to cause a decrease in Mup1-pHl fluorescence at the plasma membrane. The decrease in fluorescence does not appear to be due to endocytosis, as there are no internal Mup1-pHl structures visible, as seen in cells that are competent for endocytosis. One possibility is auxin-dependent changes in cytosolic pH; however, the reason for this decrease is unknown.

Endocytic patch initiation is independent of Pan1, whereas later steps require Pan1

To determine how CME is affected by the absence of Pan1, we tagged several known endocytic proteins with fluorescent markers and observed their patch dynamics in the Pan1-AID strain after

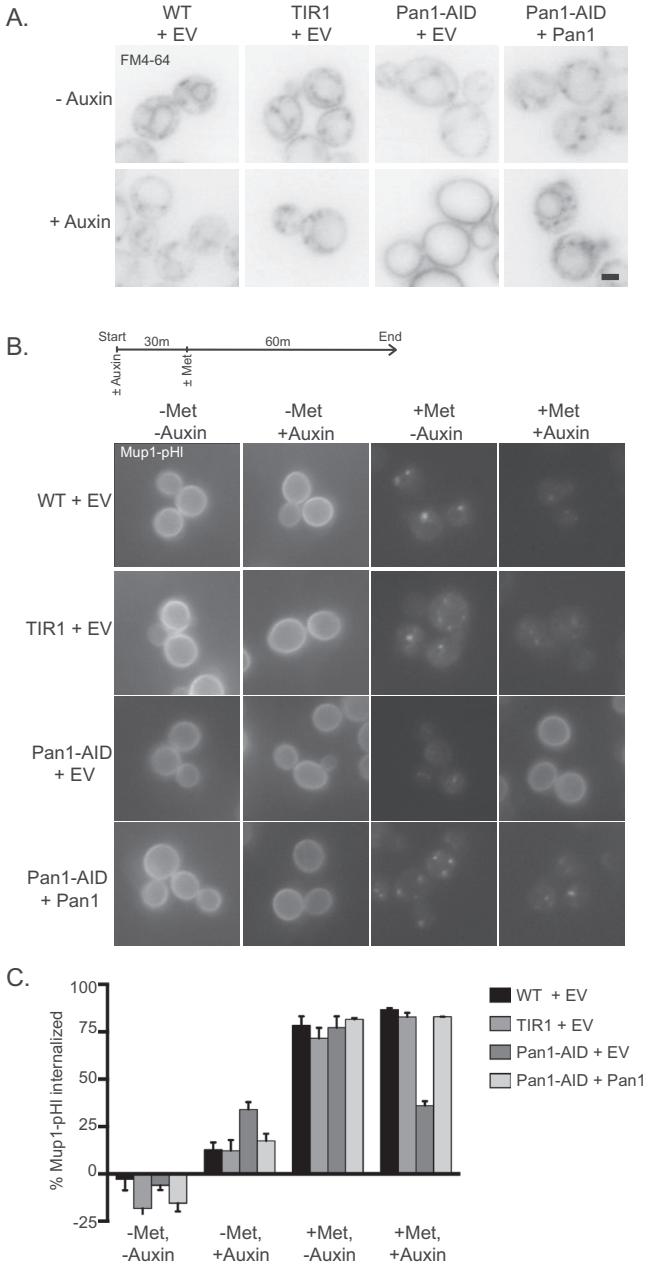

FIGURE 2: Bulk and receptor-mediated endocytosis is arrested in Pan1-AID in the presence of auxin. (A) Representative images of log-phase cultures grown ± auxin for 30 min before labeling with FM4-64 for 15 min. (B) Representative images of log-phase cultures ± pretreatment with auxin for 30 min, followed by addition of methionine for 1 h. Schematic of Mup-pHl experimental time line. (C) Quantification of Mup1-pHl fluorescence internalized after 30 min ± auxin pretreatment and 1 h ± methionine. Percentage Mup1-pHl internalized was calculated by measuring the amount of fluorescence at the end of the assay compared with the amount at the beginning. Average of three replicate experiments (mean ± SD). Scale bar, 2 μm.

45–60 min in the absence or presence of auxin. For all proteins tested, lifetimes and patch dynamics in control strains (WT and TIR1) in the presence and absence of auxin, as well as in Pan1-AID in the absence of auxin, were similar to previously published results (Tables 1 and 2 and Supplemental Figure S1, A and B; Gagny *et al.*, 2000; Kaksonen *et al.*, 2003, 2005; Barker *et al.*, 2007; Stimpson *et al.*, 2009). This indicates that addition of auxin, AID tag, or TIR1 did not affect endocytic dynamics when applied individually. Therefore any patch number or lifetime discrepancies between Pan1-AID cells incubated in the presence or absence of auxin would suggest that Pan1 has a role in that protein's recruitment and regulation at the endocytic patch. If a protein localized to the patch and had a similar patch lifetime in Pan1-AID cells plus auxin, this would indicate that Pan1 was not required for that protein's recruitment and regulation at the patch.

Pan1 is not required to initiate early events in endocytosis

We first present our findings pertaining to the proteins that arrive before Pan1 at the endocytic patch. In Pan1-AID plus auxin cells, Ede1-GFP was observed in patches that were stable for at least 6 min, the length of the image acquisition period (Tables 1 and 2 and Figure 3, A–D). In WT cells, Ede1-GFP binds and colocalizes with several endocytic proteins, including Pan1, and then dissociates from the endocytic patch before recruitment of actin (Gagny *et al.*, 2000; Stimpson *et al.*, 2009). In Pan1-AID plus auxin, Sac6-RFP actin patches and flares did not overlap with Ede1-GFP patches even though the Ede1 patches were stable, suggesting that the early and late coat may have become unlinked (Figures 3D and 4B and Supplemental Movie S1). The adaptor proteins Yap1801 and Ent2 both arrive to the patch before Pan1 and bind to Pan1's second EH domain (Wendland and Emr, 1998; Wendland *et al.*, 1999). In Pan1-AID plus auxin, Yap1801-GFP and Ent2-GFP had increased lifetimes relative to controls, and 26 and 50% of patches, respectively, remained stable for the duration of image acquisition (Tables 1 and 2 and Figure 3, A and B).

Sla2, a coat/adaptor protein, is believed to arrive slightly before Pan1 at the patch and binds several endocytic proteins, including Pan1's central region (Toshima *et al.*, 2007). In Pan1-AID plus auxin, Sla2-GFP had an increased lifetime relative to controls, with 44% of patches remaining stable for the duration of image acquisition (Tables 1 and 2 and Figure 3, A–C). Although Sla2-GFP was recruited to patches, there were slightly fewer Sla2-GFP patches in the presence of auxin (Table 2 and Figure 3B). Similar to WT cells, Sla2-GFP patches that were not stable moved in with the patch (Figure 3C).

Progression of the endocytic coat from early to late stages is dependent on Pan1

The remaining coat and actin proteins we observed all arrive at endocytic patches at the same time or after Pan1 in WT cells. In Pan1-AID plus auxin, Sla1, End3, Las17, Myo5, Rvs167, and Sac6 had decreased numbers of patches, and all except Rvs167 had increased lifetimes at the patch relative to controls (Tables 1 and 2 and Figure 3, A–D). Previous work showed a decrease in patch number and an increase in Myo5 lifetime upon deletion of Pan1's proline-rich domain, to which Myo5 binds (Barker *et al.*, 2007). Sla1, End3, and Myo5 bind Pan1, but they localized to endocytic patches in the absence of Pan1, so their localization to patches must depend on their interactions with other proteins and/or the membrane (Tang *et al.*, 1997, 2000; Barker *et al.*, 2007; Whitworth *et al.*, 2014). Las17 and Rvs167 are not known to bind Pan1 directly and were also able to localize independently of Pan1. In patches that did not result in actin flares (see later discussion), Sla2, Sla1, and End3 internalized with the patch, whereas Myo5, Las17, and Rvs167 remained at the plasma membrane in a manner comparable to a wild-type endocytosis event.

Pan1 is required for proper actin polymerization dynamics at the patch

Pan1's C-terminus is believed to contribute to actin polymerization at endocytic patches via several actin-regulatory domains and direct

	Lifetime (mean ± SD)					
	Wild type		TIR1		Pan1-AID	
Protein	–Auxin	+Auxin	–Auxin	+Auxin	–Auxin	+Auxin
Ede1	77.5 ± 32.8	83.5 ± 34.2	82.4 ± 28.3	84.0 ± 30.5	82.4 ± 29.5	360 + (stable)
Yap1801	42.5 ± 10.9	44.2 ± 12.9	44.9 ± 13.6	43.3 ± 12.1	43.2 ± 11.6	67.9 ± 29.2
Ent2	54.7 ± 13.8	56.5 ± 16.2	54.1 ± 16.3	54.6 ± 12.8	53.2 ± 13.8	161.6 ± 66.2
Sla2	34.8 ± 9.0	40.1 ± 11.2	38.0 ± 10.7	40.7 ± 10.0	36.5 ± 9.9	98.6 ± 47.8
Sla1	27.8 ± 6.2	30.6 ± 7.0	27.5 ± 6.4	31.4 ± 5.6	25.1 ± 6.6	36.3 ± 17.7
End3	29.8 ± 6.8	32.8 ± 7.5	28.5 ± 6.3	29.9 ± 7.4	27.9 ± 6.0	42.5 ± 14.0
Las17	32.0 ± 8.1	34.3 ± 8.9	28.6 ± 6.7	32.1 ± 8.6	31.6 ± 9.4	60.7 ± 39.7
Myo5	10.3 ± 2.1	10.6 ± 2.2	10.4 ± 1.5	10.1 ± 1.9	9.5 ± 2.0	12.5 ± 6.7
Rvs167	11.2 ± 3.1	9.4 ± 2.3	9.9 ± 2.9	8.5 ± 2.4	10.0 ± 2.9	8.8 ± 3.9
Sac6	13.6 ± 3.8	13.4 ± 3.5	12.0 ± 2.7	14.5 ± 3.4	12.5 ± 3.9	23.3 ± 14.3 (total)
						16. 8 ± 5.3 (patches)
						42.8 ± 15.1 (flares)

TABLE 1: Endocytic patch lifetime(s) of fluorescently tagged proteins.

binding to F-actin (Duncan *et al.*, 2001; Toshima *et al.*, 2005). In Pan1-AID cells plus auxin, we observed a significant decrease in the number of actin patches (Sac6–red fluorescent protein [RFP] was used to label branched F-actin); those that formed had an increased lifetime, and some patches had the appearance of elongated structures of polymerized actin, which were named "actin flares" (Tables 1 and 2, Figure 4, A–D, and Supplemental Movies S1–S3). These actin flares originated from an endocytic patch and extended into the cytoplasm, sometimes flowing parallel to the plasma membrane. The coat components Sla2, Sla1, and End3 moved with the tip of the actin flare. To visualize plasma membrane dynamics in relation to the actin flares, we used GFP–pleckstrin homology domain chimeras (GFP-PH), which bind the phosphatidylinositol (4,5)-bisphosphate lipids found in abundance on the plasma membrane. As a control, we confirmed that GFP-PH does label internalized membrane in synaptojanin mutants, as seen in previous work (Supplemental Figure S1C; Stefan *et al.*, 2002). The Pan1-AID actin flares did not contain membrane (Figure 4C and Supplemental Movie S3), suggesting the coat/actin machinery has weakened connections to the membrane. These flares differed from the aberrant actin phenotypes observed previously in other endocytic mutants. The actin-uncoupling phenotype observed in *sla2*Δ or *ent1/2*Δ cells is characterized by short actin comet tails anchored at the plasma membrane that do not invaginate the plasma membrane or coat components (Kaksonen *et al.*, 2003; Skruzny *et al.*, 2012). In contrast, the uncontrolled Arp2/3 actin plumes seen in *sla1*Δ*/bbc1*Δ or *end3*Δ*/bbc1*Δ cells are long and contain invaginated plasma membrane with coat components at the tip (Kaksonen *et al.*, 2005). In Pan1-AID plus auxin, the actin flares were not stable at patches, contained the coat components Sla2, Sla1, and End3, but did not contain membrane

	Patch number per micrometer of plasma membrane (mean ± SD)					
	Wild type		TIR1		Pan1-AID	
Protein	–Auxin	+Auxin	–Auxin	+Auxin	–Auxin	+Auxin
Ede1	0.87 ± 0.3	0.84 ± 0.1	0.85 ± 0.2	0.79 ± 0.1	0.80 ± 0.2	0.84 ± 0.2
Yap1801	0.35 ± 0.1	0.37 ± 0.1	0.33 ± 0.1	0.35 ± 0.1	0.36 ± 0.1	0.34 ± 0.1
Ent2	0.30 ± 0.1	0.29 ± 0.1	0.32 ± 0.1	0.33 ± 0.1	0.31 ± 0.1	0.31 ± 0.1
Sla2	0.57 ± 0.1	0.60 ± 0.1	0.54 ± 0.1	0.55 ± 0.1	0.51 ± 0.1	0.40 ± 0.1
Sla1	0.36 ± 0.1	0.36 ± 0.1	0.37 ± 0.1	0.34 ± 0.1	0.32± 0.1	0.10 ± 0.1
End3	0.60 ± 0.2	0.54 ± 0.1	0.53 ± 0.1	0.56 ± 0.1	0.50 ± 0.1	0.07 ± 0.1
Las17	0.41 ± 0.1	0.41 ± 0.1	0.44 ± 0.1	0.40 ± 0.1	0.36 ± 0.1	0.10 ± 0.1
Myo5	0.22 ± 0.1	0.21 ± 0.1	0.22 ± 0.1	0.21 ± 0.1	0.23 ± 0.1	0.08 ± 0.1
Rvs167	0.32 ± 0.1	0.34 ± 0.1	0.28 ± 0.1	0.24 ± 0.1	0.33 ± 0.1	0.07 ± 0.1
Sac6	0.28 ± 0.1	0.23 ± 0.1	0.29 ± 0.1	0.25 ± 0.1	0.27 ± 0.1	0.07 ± 0.1 (total)
						0.08 ± 0.1 (patches)
						0.01 ± 0.01 (flares)

TABLE 2: Endocytic patch number per micrometer of plasma membrane of fluorescently tagged proteins.

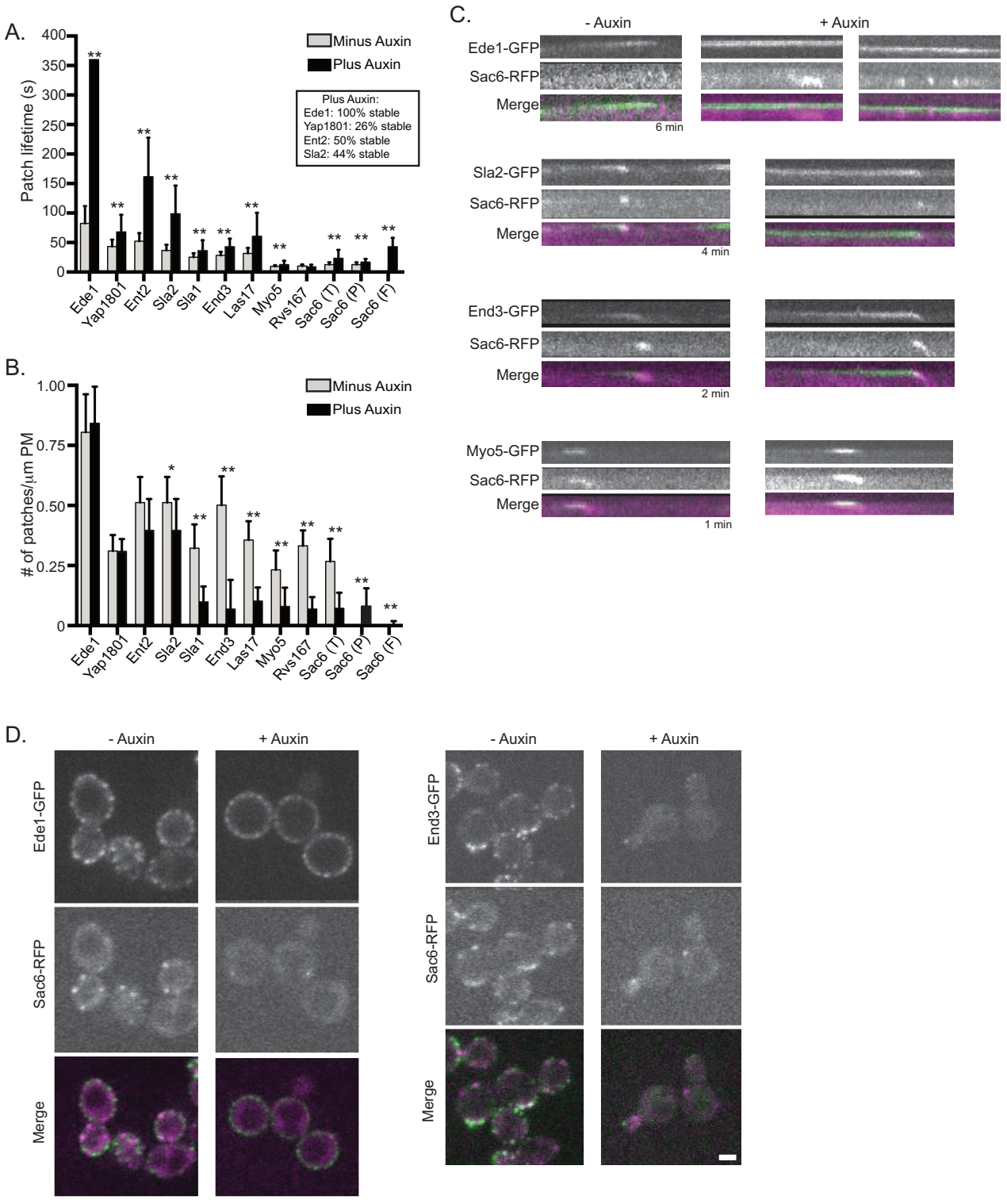

FIGURE 3: Endocytic proteins tagged with GFP have altered dynamics in Pan1-AID in the presence of auxin. (A) Patch lifetime (seconds) and (B) number of patches per micrometer of plasma membrane of endogenously GFP- and RFP-tagged proteins in Pan1-AID cells after 45–60 min ± auxin. Movies were taken with intervals of 0.5–4 s, 90–120 frames, with an exposure of 150 ms. For lifetimes, >50 patches/strain, and percentage stable is the number of patches that remained present for the entire duration of image acquisition. For patch numbers, >30 cells/strain. Sac6-RFP is split into patches (P), flares (F), and total (T) Sac6-RFP structures. *$p \leq 0.001$, **$p \leq 0.0001$, minus vs. plus auxin (mean ± SD). (C) Representative kymographs of GFP-tagged proteins and Sac6-RFP in Pan1-AID cells grown ± auxin for 45–60 min. All kymographs are oriented with cell interior at the bottom. Kymographs made from movies used for the quantification. (D) Images of representative cells from Pan1-AID strains grown ± auxin for 45–60 min. Scale bar, 2 μm.

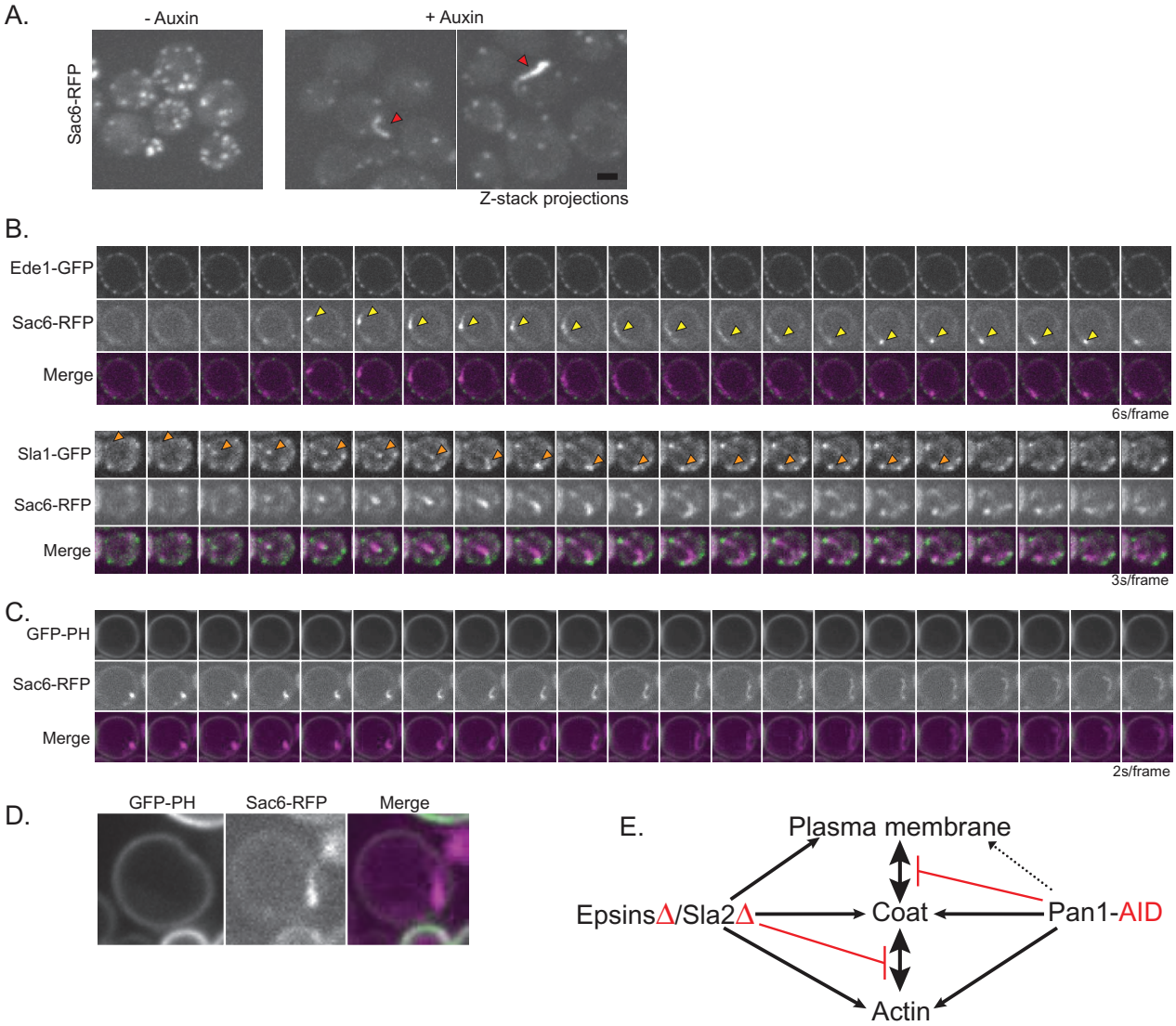

FIGURE 4: Dynamic actin flares appear in Pan1-AID cells in the presence of auxin. (A) *Z*-stack projections (maximum intensity) of Sac6-RFP Pan1-AID cells grown ± auxin for 45–60 min. Intervals of 0.27 µm. Red arrow, Sac6-RFP flare. (B) Time series of movies of Pan1-AID cells with indicated GFP/RFP proteins grown plus auxin for 45–60 min. Yellow arrow, Sac6-RFP flare moving along the PM without overlapping Ede1-GFP. Orange arrow, Sla1-GFP patch moving into the cell with a Sac6-RFP flare. Scale bar, 2 µm. (C) Time series of movies of Sac6-RFP Pan1-AID cells with GFP-PH plasma membrane label; grown plus auxin for 45–60 min. (D) Representative image of Sac6-RFP Pan1-AID cells with GFP-PH plasma membrane label; grown plus auxin for 45–60 min. (E) Model of Pan1 and Epsins/Sla2 interactions with the plasma membrane, endocytic coat, and actin machinery. *epsinΔ/sla2Δ* and Pan1-AID phenotypes shown in red. Dashed arrow represents binding between Pan1 and lipids (D. Pierce and B. Wendland, unpublished data).

(Figure 4, A–D, and Supplemental Movies S1–S3). The Pan1-AID actin flares were longer than the *sla2Δ* or *ent1/2Δ* actin comet tails but not as elongated as the actin plumes seen in *sla1Δ/bbc1Δ* or *end3Δ/bbc1Δ*. It is known that Pan1 binds several actin regulators, such as the Las17 inhibitor Sla1 and the Arp2/3 activators Myo3 and Myo5 (Tang *et al.*, 2000; Duncan *et al.*, 2001; Toshima *et al.*, 2005; Barker *et al.*, 2007). Our data suggest that Pan1 may be involved in the coordination of actin regulatory elements at the patch and is important for proper linkage of the coat to the membrane in order to transmit the force of actin polymerization needed to invaginate the membrane (Figure 4E).

To briefly summarize our findings in Pan1-AID cells plus auxin, the endocytic factors that arrive before Pan1 (Ede1, Ent2, Yap1801, and Sla2) had longer lifetimes, with some of the patches remaining stable for the duration of the data collection period (Table 1 and Figure 3, A–D). The CME components that arrive at the same time as or after Pan1 (Sla1, End3, Las17, Myo5, Rvs167, and Sac6) also had increased lifetimes, whereas, unlike the earlier-arriving proteins, they had decreased patch numbers (Tables 1 and 2 and Figure 3, A–D). Overall longer lifetimes and fewer late coat patches suggested inefficient progression of the endocytic patch to later stages and fewer productive endocytic events. The most dramatic phenotypic difference observed in the Pan1-AID strain in the presence of auxin (relative to the absence of auxin) was a significant decrease in the number of Sac6-RFP patches and the appearance of actin flares as labeled by Sac6-RFP (Figure 4, A–D). These flares contained late

coat proteins but not membrane and are thus believed not to be successful sites of endocytosis (Figure 4, A–D).

A portion of Pan1's N-terminal and central regions is critical for patch localization and its endocytic and essential functions

Pan1's central region is critical for localization and stabilization at endocytic patches. We predicted that Pan1 must localize to the patch in order to perform its endocytic function. We identified the regions of Pan1 that are critical for proper Pan1 localization to the endocytic patch by C-terminally tagging Pan1 fragments with GFP and observing their localization. Pan1 binds several other endocytic proteins, some of which arrive to the patch before Pan1 and may recruit Pan1. Pan1 also binds itself, so by expressing the fragments in the Pan1-AID strain in the absence and presence of auxin, we were able to determine whether the presence of full-length Pan1 was necessary for proper localization of the fragments (Miliaras and Wendland, 2004; Toshima *et al.*, 2005; Pierce *et al.*, 2013). All Pan1 fragments used expressed protein of expected size in both the absence and presence of auxin (Supplemental Figure S2).

All Pan1-GFP fragments tested were able to localize to endocytic patches in the absence and presence of auxin except for Pan1AA402-855-GFP and Pan1AA1050-1480-GFP (Figure 5, A–C, and Supplemental Figure S3A). This confirmed that the C-terminal actin regulatory region of Pan1 was not necessary for localization and could not localize to patches without the in-*cis* support of the central region. The N-terminal (Pan1AA1-702-GFP) and central region (Pan1AA702-1050-GFP) were individually sufficient to localize to the patches. Both the N-terminal and central regions of Pan1 have endocytic binding partners that arrive before or at the same time as Pan1 to patches, suggesting that these interactions may be important for Pan1's recruitment to patches.

In the absence of auxin, Pan1-GFP fragments had a decreased patch number and lifetime compared with full-length Pan1. On removal of full-length Pan1 by the addition of auxin, all Pan1-GFP fragments (except Pan1AA702-1050-GFP) trended toward more patches; this increase was significant for Pan1AA1-855-GFP, AA250-855-GFP, and AA402-1050-GFP (Figure 5, A–C). This suggests that these fragments were competing with full-length Pan1 for binding at the patch. The lifetimes of all fragments also increased in the presence of auxin; this may be due to decreased competition with full-length Pan1 and/or an overall increase in endocytic patch lifetime observed in Figure 3.

Although a majority of Pan1 fragments were able to localize to endocytic patches, some had significantly decreased lifetimes at the patch compared with full-length Pan1 (Figure 5A). There are several interpretations for the shortened lifetimes, one of which is that these fragments are missing key binding elements that strengthen Pan1's interactions at the patch. Similar to Pan1 localization, Pan1's central region was critical for Pan1 fragment stabilization/lifetime at the patch, as highlighted by the dramatic difference in lifetime and patch number between Pan1AA1-702 and Pan1AA1-855/1050. Although Pan1AA1-702-GFP and Pan1AA1-855/1050-GFP can both localize to patches, AA1-702-GFP had a significantly shorter lifetime, suggesting that Pan1AA703-855/1050 contains a patch-stabilizing property. However, the central region alone, Pan1AA702-1050-GFP, also had a short lifetime, indicating that this region required another Pan1 region for normal temporal behavior. Additional N- or C-terminal sequences appended to the Pan1AA702-1050-GFP fragments increased its lifetime, but only the addition of the N-terminus increased the lifetime to WT levels. Therefore the N-terminal and central regions together restore normal lifetime dynamics of Pan1 at endocytic patches.

In conclusion, the central region (Pan1AA702-1050) alone was sufficient for Pan1 localization to the endocytic patch, but the N-terminus was needed to ensure that Pan1 had normal lifetime dynamics.

Pan1's EH domains and central region are necessary for its endocytic function. In the absence of full-length Pan1, endocytosis was arrested (Figure 2). We identified the regions of Pan1 necessary for its endocytic role using the Mup1-pHl assay with Pan1 fragments in the Pan1-AID strain. After pretreatment with auxin for 30 min, methionine was added to induce internalization of Mup1-pHl, and cells were observed 1 h later. If a Pan1 fragment contained all regions necessary for endocytosis, Mup1-pHl would be efficiently internalized, and the cells would be dim, similar to cells with full-length Pan1. However, if a Pan1 fragment could not support endocytosis, Mup1-pHl would remain at the plasma membrane, and the cells would be bright, similar to Pan1-AID cells with EV. In the case where an intermediate brightness value of the population was obtained, there are two potential explanations. First, there may be a mixture of cells with Mup1-pHl at the plasma membrane, in endosomes or MVBs, or dim in the vacuole, part of which may be due to heterogeneous expression of plasmids from cell to cell. Alternatively, this could be due to all the cells having an overall intermediate brightness. When quantified for percentage of Mup1-pHl internalized, these samples would have values between those seen for EV and for full-length Pan1. An intermediate phenotype is indicative of slow or inefficient endocytosis, suggesting the fragment only partially restored endocytosis.

Similar to results for Pan1 localization, efficient Mup1-pHl internalization required Pan1's central region supported by portions of the N-terminus; the C-terminal actin region was not required (Figure 5, D and E, and Supplemental Figure 3, B and C). It was previously believed that Pan1's first EH domain was less important for Pan1's endocytic role, as it does not bind adaptor proteins and was found to be dispensable for viability (Sachs and Deardorff, 1992; Wendland and Emr, 1998; Wendland *et al.*, 1999). Surprisingly, we found that the first EH domain could in fact support endocytosis in the absence of EH2, as Pan1AA1-390, 680-1490 internalized most Mup1-pHl (Figure 5, D and E, and Supplemental Figure S3, B and C). However, when both EH domains were deleted, as in Pan1AA1-97, 680-1480, Mup1-pHl was not internalized. Although the N-terminus of Pan1 (Pan1AA1-702) could localize to endocytic patches, this region was unable to promote internalization of Mup1-pHl. Extending the fragment to include some of the central region (Pan1AA1-855) restored the endocytic function, further confirming Pan1's central region as critical for Pan1's localization and function at the endocytic patch. In addition, we defined a region of Pan1, AA402-855, that was necessary but not sufficient for endocytosis, as Pan1AA1-401, 856-1480 and AA402-855 did not internalize Mup1-pHl. This region spans the EH2 domain and some of the central region. Of interest, adding to this AA402-855 fragment either the rest of the central region (Pan1AA402-1050) or the N-terminus (Pan1AA1-855) restored the endocytic function. Pan1AA250-855, which includes both EH domains, only barely restored endocytosis (as seen by the punctae present in Figure 5E), whereas the far-N-terminal portion of LR1 (Pan1AA1-97, 402-855) did not promote internalization of Mup1-pHl at all. These data suggest that Pan1AA402-855 is critical for CME, but it requires LR1 (including EH1) or the rest of the central region for full endocytic function.

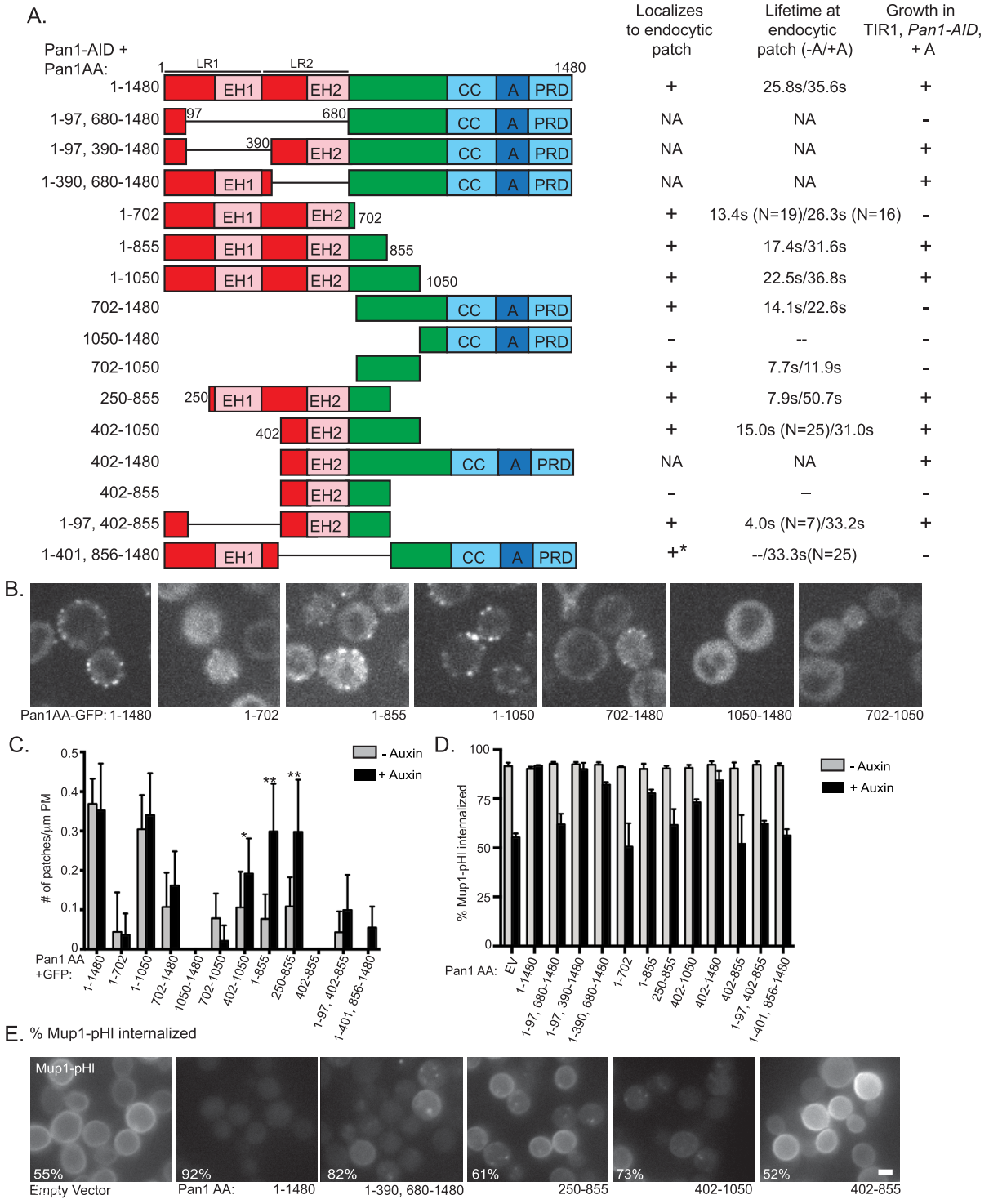

FIGURE 5: Pan1's central region is critical for endocytic function and viability. (A) Schematic of Pan1 and Pan1-GFP fragments. C-terminally GFP-tagged protein localization to endocytic patch: +, localizes to patch; –, no patches present; *only localizes when auxin present. Lifetime(s) of GFP-tagged proteins at endocytic patch ± auxin for 1 h, >50 patches for all except those indicated; movies were taken with 1-s frames for 120 frames, 150-ms exposure. Rescue of growth of Pan1-AID by Pan1 protein fragments in the presence of auxin: +, rescue, –, no rescue. (B) Representative images of Pan1-AID cells plus indicated Pan1-GFP fragments grown in the presence of auxin for 1 h. (C) Number of Pan1-GFP patches per micrometer of plasma membrane in Pan1-AID strain ± auxin for 1 h. No patches were observed for Pan1 AA1050-1480-GFP and Pan1AA402-855-GFP; >30 cells/strain. *$p \leq 0.01$, **$p \leq 0.0001$ minus vs. plus auxin (mean ± SD). (D) Amount of Mup1-pHl internalized in Pan1-AID strains plus indicated plasmids after 30 min ± auxin and 1 h plus methionine. Percentage Mup1-pHl internalized was calculated by measuring the amount of fluorescence at the end of the assay compared with the amount at the beginning. Average of three replicate experiments (mean ± SD). (E) Representative images of Pan1-AID strains plus indicated plasmids after 30 min plus auxin and 1 h plus methionine. Percentage is average Mup1-pHl internalized calculated in C. Scale bar, 2 μm.

In summary, Pan1AA402-855, which contains EH2 and a portion of the central region, was critical for endocytic function and patch formation and requires either LR1 or the central region for full restoration of endocytic defects.

Pan1 contains three overlapping minimal essential fragments that localize to patches, but only one restores endocytosis. Pan1 is an essential protein whose primary role is in CME, which is not believed to be an essential process; therefore this raises the question of Pan1's essential role and whether can it be separated from its role in endocytosis. To explore these questions, we defined the essential regions of Pan1 by expressing fragments of Pan1 on plasmids in Pan1-AID cells and observing which fragments restored growth and viability in the presence of auxin. Pan1 AA402-855 is necessary but not sufficient for growth or viability; this "minimal" essential region requires the addition of one of three regions of Pan1—AA250-401, AA856-1050, or AA1-97—to rescue growth and viability (Figure 5A and Supplemental Figure S4A). The minimal region contains the second EH domain, as well as a portion of the central region that is important for Pan1-Pan1 binding and Pan1-End3 binding. Pan1's C-terminal actin-regulatory region is not essential for viability, confirming data from the literature (Duncan *et al.*, 2001).

In addition, we found that Pan1's first EH domain could support growth in the absence of the second EH domain (and vice versa), contradicting previous results (Figure 5A and Supplemental Figure S4A; Sachs and Deardorff, 1992). This disparity was resolved by our finding that the original plasmid does not express protein. Adaptor proteins have been shown to bind only the second EH domain; however, our data suggest that either adaptor proteins can interact with the first EH domain or these interactions are not essential for growth or endocytosis.

All Pan1 fragments tested that did not support growth also did not restore viability of the Pan1-AID strain in the presence of auxin (Supplemental Figure S4B). The essential regions of Pan1 partially restored viability, but the increased death suggests that the cells are in a compromised state, perhaps due to partial loss of Pan1's nonessential function.

In summary, Pan1's minimal common region, AA402-855, is critical for its localization and stability at the endocytic patch and necessary for Pan1's endocytic and essential roles. This common region requires additional Pan1 regions to stably localize to endocytic patches (Pan1AA1-97, AA250-401, or AA856-1050), restore endocytosis (Pan1AA1-401 or AA856-1050), or support cell viability (Pan1AA1-97, AA250-401, or AA856-1050). The exact mechanism of action that each of these three regions contributes to the common essential region is under investigation. Of the Pan1 fragments tested, all fragments that did not support growth also did not restore endocytosis or viability. Pan1AA1-855 and Pan1AA402-1050 are the minimal regions necessary for endocytosis, but the mechanism of how either the addition of the LR1 and LR2 or the remaining central region function to restore endocytosis is unknown. Potential explanations are that the Sla1-binding site in LR1 and the lipid-binding activity in the central region could be critical for Pan1's endocytic functions (Tang *et al.*, 2000; D. Pierce and B. Wendland, unpublished results). Two fragments, Pan1AA1-97, 402-855 and Pan1AA250-855, supported growth but were not able to fully restore endocytosis of Mup1-pHl, suggesting that either 1) these fragments support a basal level of bulk endocytosis but not endocytosis of the specific cargo, or 2) these fragments have an additional, essential, role in the cell.

DISCUSSION

Pan1 interacts with numerous proteins at each stage of endocytosis, making Pan1 an ideal candidate as a scaffold to hold the coat together as it transitions between stages (Sachs and Deardorff, 1992; Wendland *et al.*, 1996). Pan-AID provided a unique opportunity to characterize endocytosis and deduce Pan1's mechanisms of endocytic regulation in the acute absence of Pan1. Pan1-AID also allowed us to characterize which regions of Pan1 are important for its endocytic and essential functions, which we found can be separated.

A majority of Pan1 protein is depleted within 1 h after the addition of auxin, yet most cells remain viable; it requires 4 h for >50% of the cells to die (Figure 1, B and F). Pan1's major role is in CME, which is not essential, so how are Pan1-AID cells dying (Payne *et al.*, 1988; Chu *et al.*, 1996; Madania *et al.*, 1999; Kaksonen *et al.*, 2005; Newpher and Lemmon, 2006; Prosser *et al.*, 2011)? We continue to pursue Pan1's essential role.

Pan1 is not required to initiate endocytic patches but is important for coat maturation. The few late coat patches that formed in the absence of Pan1 had extended lifetimes (Tables 1 and 2 and Figure 3, A and B). The decrease in the number of late coat protein patches could be due to reduced binding efficiency of individual proteins and/or fewer endocytic patches maturing to later stages. If the latter were true, this implicates Pan1 as a critical regulator of the transition from early to late coat, where Pan1 strengthens interactions that link early coat and late coat proteins (i.e., Ede1-Pan1, Syp1-Las17, Sla2-late coat proteins, and actin). Recent work identified Ede1 as an organizer of the initiation of endocytosis and suggested that Ede1's coiled-coil region binds unknown late coat protein(s) (Boeke *et al.*, 2014). Ede1's homologue, Eps15, binds Intersectin through its coiled-coil region, similar to our unpublished work that found that Pan1 binds to Ede1's coiled-coil region (Sengar *et al.*, 1999; Wong *et al.*, 2012, S. Barker and B. Wendland, unpublished observations). Together these results strongly suggest that Pan1 and Ede1 likely work together to mediate endocytic progression from early to late stages.

Although Pan1's direct role in actin regulation may be small, its indirect role in the coordination of other actin inhibitors and regulators is important (Duncan *et al.*, 2001; Toshima *et al.*, 2005; Barker *et al.*, 2007). Actin flares represent a distinct intermediate phenotype relative to the previously described actin comet tails and actin plumes seen in other endocytic mutants (Kaksonen *et al.*, 2003, 2005; Skruzny *et al.*, 2012). We hypothesize that in the absence of Pan1, early-acting inhibitors of Arp2/3-actin polymerization, such as Syp1 and Sla1, cannot properly engage Las17. This leads to increased Arp2/3 actin polymerization that resembles *sla1Δ/bbc1Δ* actin plumes (Kaksonen *et al.*, 2005). Similar to Sla2, we propose that Pan1 is critical for coupling the membrane to the coat/actin machinery in order to transmit the forces of actin polymerization to invaginate the membrane (Figure 4E; Kaksonen *et al.*, 2003; Skruzny *et al.*, 2012).

We found that the most functionally important region of Pan1, AA702-1050, is the least studied, leaving many questions open concerning mechanisms of Pan1 function. The known activities and interesting features of this region include homodimerization, End3 binding, Sla2 binding, a Prk1 consensus phosphorylation site, a lipid-binding region, and a putative NLS domain, many of which show conservation among fungal species (Tang *et al.*, 2000; Zeng *et al.*, 2001; Miliaras and Wendland, 2004; Toshima *et al.*, 2005, 2007; Kamińska *et al.*, 2007; Pierce *et al.*, 2013, D. Pierce and B. Wendland, unpublished observations). In addition, there appear to be two other areas (AA855-892 and AA918-975) that are well conserved among fungal species but have no assigned function. More careful functional study of Pan1's central region is clearly warranted.

Our work clearly shows that EH1 function supports endocytosis and viability in lieu of EH2 (Figure 5, A, D, and E, and Supplemental Figures S3 and S4). Suzuki *et al.* (2012) showed that specific deletion of both Pan1 EH1 and EH2 does not abolish endocytosis, but our data show that a fragment missing EH1, EH2, and the region between (LR2) does abolish the endocytic and essential function of Pan1; this implicates a role for the LR2 region. The only known functional features in LR2 are 10 Prk1/Ark1 phosphorylation sites (Tang *et al.*, 2000; Zeng *et al.*, 2001; Toshima *et al.*, 2005, 2007). Are these sites critical for Pan1 function, or are there unknown binding partners of the LR2? In addition, the necessity of the NPF-motif binding activity of the EH domains, in the context of the minimal essential fragments, is under investigation.

We found that the N-terminal and central regions of Pan1 independently localized to patches; each region interacts with proteins that arrive at the patch before or with Pan1, suggesting that these interactions contribute to Pan1 recruitment (Tang *et al.*, 1997, 2000; Wendland and Emr, 1998; Wendland *et al.*, 1999; Toshima *et al.*, 2007). Of interest, some fragments, such as Pan1AA1-702 and 1-97, 402-855, localized to the patch without supporting endocytosis. This demonstrated that regions important for endocytic localization and function are separable, and these are being further studied.

Our work found two minimal fragments of Pan1 that support viability and endocytosis: Pan1AA1-855 and AA402-1050 (Figure 5 and Supplemental Figures S3 and S4). Do these two fragments support endocytosis in similar or different ways? Pan1AA855-1050 interacts with Sla2 and the membrane, both of which could help Pan1 localize to and function at endocytic patches (Toshima *et al.*, 2007; D. Pierce and B. Wendland, unpublished observations). In contrast, Pan1AA1-402, which contains LR1, EH1, and part of LR2, could help localize Pan1 to the patch through Sla1 interactions or phosphoregulation. That Pan1AA250-855 and Pan1AA1-97, 402-855 do not support endocytosis suggests an endocytic role for LR1, perhaps via Sla1 binding (Tang *et al.*, 2000; Zeng *et al.*, 2001; Toshima *et al.*, 2005, 2007). The exact binding domain of Sla1 needs to be defined to determine whether Pan1-Sla1 interaction is critical for endocytosis.

Of interest, we found two minimal fragments of Pan1 that support viability and localize to patches but do not fully restore endocytosis: Pan1AA250-855 and Pan1AA1-97, 402-855 (Figure 5 and Supplemental Figures S3 and S4). Pan1AA250-402 contains EH1 and LR2, whereas the other has a glutamine-rich N-terminus with an NPY motif. How are these regions contributing to Pan1's essential function? Are the EH domains important for viability? Are there non-endocytic proteins that interact with Pan1 in these regions? Is Pan1's essential function carried out at the endocytic patch? We are continuing to define Pan1's essential and endocytic functions.

Our study of Pan1 confirmed that Pan1 is an essential endocytic scaffold and defined this function as regulating interactions important for transitions between endocytic stages: the early coat to the late coat, actin-regulatory proteins to actin machinery, and the membrane to the coat/actin machinery. We also defined the regions of Pan1 that are important for endocytosis and, for the first time, found regions of Pan1 that do not support endocytosis but do support viability. Pan1-AID will allow us to continue defining Pan1's acute functions in endocytosis and its unknown role(s).

MATERIALS AND METHODS

Media and growth conditions

Yeast cells were grown in rich (yeast extract/peptone) or synthetic (yeast nitrogenous base with amino acid selection of plasmid maintenance) medium with 2% dextrose. For experiments using auxin in liquid cultures, 3-indoleacetic acid (I2886; Sigma-Aldrich, St. Louis, MO) was added to synthetic media to a final concentration of 500 µm. For experiments using auxin on solid media, 1-naphthaleneacetic acid (NAA; N0640; Sigma-Aldrich) was added to synthetic media to a final concentration of 1 mM.

Strains and plasmids

The yeast strains and plasmids used in this study are listed in Tables 3 and 4, respectively. Strains were constructed using PCR-based genomic integration as described previously (Longtine *et al.*, 1998; Goldstein and McCusker, 1999; Nishimura *et al.*, 2009). DNA manipulations for plasmid construction were performed using standard techniques, using either T4 DNA polymerase-mediated ligations in *Escherichia coli* or homologous recombination with overlapping DNA fragments followed by plasmid rescue in *Saccharomyces cerevisiae*. All restrictions enzymes were purchased from New England Biolabs (Ipswich, MA).

Protein expression

Trichloroacetic acid precipitation. Mid to late log-phase cells without or with auxin at indicated time points were harvested and resuspended in 1 ml of 10% trichloroacetic acid with 1 mM 4-(2-aminoethyl)benzenesulfonyl fluoride (AEBSF; a protease inhibitor) and incubated on ice for 20 min, and precipitates were centrifuged at 14,000 rpm for 10 min at 4°C. Precipitates were washed twice with cold acetone, resuspended by sonication, and air dried. Protein samples were processed for SDS–PAGE separation by adding 2× protein sample buffer with 1 mM AEBSF and solubilized by bead disruption.

SDS–PAGE and immunoblotting. Proteins were separated on polyacrylamide mini gels (7.5%) at 27 mA in SDS running buffer (3 mM SDS, 25 mM Tris base, 192 mm glycine) and then transferred onto nitrocellulose membranes at 80 V for 90 min in cold transfer buffer (20% methanol, 0.0375% SDS, 48 mM Tris base, 30 mM glycine). The membranes were blocked in 5% milk in TBST (10 mM Tris, pH 7.5, 0.25 M NaCl, 0.025% Tween-20). Blots were incubated in the specified primary antibody overnight at the following concentrations: rabbit-anti-Pan1 was a gift from D. G. Drubin (University of California, Berkeley) and was used at 1:10,000; rabbit-anti-Act1 was a gift from D. Pruyne (SUNY Upstate Medical University) and was used at 1:5000; rabbit-anti-End3 was a gift from the H. Riezman lab and was used at 1:2000; and rabbit-anti-Sla1 was a gift from L. Hicke (University of Texas, Austin) and was used at 1:2000. The blots were washed three times in TBST, incubated with secondary antibodies conjugated to horseradish peroxidase (Pierce, Rockford, IL), and diluted 1:2000 in milk solution for 45 min. Blots were washed again three times in TBST and then developed with chemiluminescent substrate (solution 1, 2.5 mM luminol, 400 µM paracoumaric acid, 100 mM Tris-HCl, pH 8.5; solution 2, 5.4 mM H_2O_2, 100 mM Tris-HCl, pH 8.5) for 2 min at room temperature. Chemiluminescence images were acquired using a FluorChem M FM0455 imager.

Growth assays

For serial dilutions, log-phase cells were diluted to OD_{600} of 0.25, from which four 1:5 serial dilutions were plated on yeast nitrogen base (YNB) –tryptophan minus or plus 1 mm NAA and grown for 3 d at 30°C.

Propidium iodide staining

Aliquots of cells from each culture were taken at the indicated times after incubation in minus or plus 500 µm IAA at 30°C and labeled

Strain	Genotype	Source
W303	*MATα ura3-1 ade2-1 his3-11 leu2,3112 trp1-1 can1-100 ade2::ADE2*	Laboratory strain
BY25598	*MATa ura3-1 ade2-1 his3-11, 15 leu2-3112 trp1-1 can1-100 ADH1-OsTIR1-9myc::URA3*	Yeast Genetic Resource Center
BWY1488	*MATa his3-Δ200 trp1-Δ901 leu2-3112 ura3-52 lys2-801 suc2-Δ9 BAR1 sjl1::HIS3, sjl2::HIS3*	Laboratory strain
BWY5393	*MATα ura3-1 ade2-1 his3-11, 15 leu2-3112 trp1-1 can1-100 ade2::ADE2 ADH1-OsTIR1-9myc::URA3 HisΔ::URA*	This study
BWY5394	*MATα ura3-1 ade2-1 his3-11, 15 leu2-3112 trp1-1 can1-100 ADH1-OsTIR1-9myc::URA3 ade2::ADE2 HisΔ::URA Pan1-AID::G418*	This study
BWY5890	*MATα ura3-1 ade2-1 his3-11 leu2,3112 trp1-1 can1-100 ade2::ADE2 Ade8Δ::LEU*	This study
BWY5891	*MATα ura3-1 ade2-1 his3-11, 15 leu2-3112 trp1-1 can1-100 ade2::ADE2 ADH1-OsTIR1-9myc::URA3 HisΔ::URA Ade8Δ::LEU*	This study
BWY5892	*MATα ura3-1 ade2-1 his3-11, 15 leu2-3112 trp1-1 can1-100 ade2::ADE2 ADH1-OsTIR1-9myc::URA3 HisΔ::URA Pan1-AID::G418 Ade8Δ::LEU*	This study
BWY6051	*MATα ura3-1 ade2-1 his3-11 leu2,3112 trp1-1 can1-100 ade2::ADE2 Ade8Δ::LEU Mup1-pHl::HPH*	This study
BWY6052	*MATα ura3-1 ade2-1 his3-11, 15 leu2-3112 trp1-1 can1-100 ade2::ADE2 ADH1-OsTIR1-9myc::URA3 HisΔ::URA Ade8Δ::LEU Mup1-pHl::HPH*	This study
BWY6053	*MATα ura3-1 ade2-1 his3-11, 15 leu2-3112 trp1-1 can1-100 ade2::ADE2 ADH1-OsTIR1-9myc::URA3 HisΔ::URA Pan1-AID::G418 Ade8Δ::LEUMup1-pHl::HPH*	This study
BWY6191	*MATα ura3-1 ade2-1 his3-11 leu2,3112 trp1-1 can1-100 ade2::ADE2 Ade8Δ::LEU Ent2-GFP::G418*	This study
BWY6192	*MATα ura3-1 ade2-1 his3-11, 15 leu2-3112 trp1-1 can1-100 ade2::ADE2 ADH1-OsTIR1-9myc::URA3 HisΔ::URA Ade8Δ::LEU Ent2-GFP::G418*	This study
BWY6193	*MATα ura3-1 ade2-1 his3-11, 15 leu2-3112 trp1-1 can1-100 ade2::ADE2 ADH1-OsTIR1-9myc::URA3 HisΔ::URA Pan1-AID::G418 Ade8Δ::LEU Ent2-GFP::G418*	This study
BWY6146	*MATα ura3-1 ade2-1 his3-11 leu2,3112 trp1-1 can1-100 ade2::ADE2 Ade8Δ::LEU YAP1801-GFP::G418*	This study
BWY6147	*MATα ura3-1 ade2-1 his3-11, 15 leu2-3112 trp1-1 can1-100 ade2::ADE2 ADH1-OsTIR1-9myc::URA3 HisΔ::URA Ade8Δ::LEU YAP1801-GFP::G418*	This study
BWY6148	*MATα ura3-1 ade2-1 his3-11, 15 leu2-3112 trp1-1 can1-100 ade2::ADE2 ADH1-OsTIR1-9myc::URA3 HisΔ::URA Pan1-AID::G418 Ade8Δ::LEU YAP1801-GFP::G418*	This study
BWY6054	*MATα ura3-1 ade2-1 his3-11 leu2,3112 trp1-1 can1-100 ade2::ADE2 Ade8Δ::LEURVS167-GFP::HPH*	This study
BWY6055	*MATα ura3-1 ade2-1 his3-11, 15 leu2-3112 trp1-1 can1-100 ade2::ADE2 ADH1-OsTIR1-9myc::URA3 HisΔ::URA Ade8Δ::LEU RVS167-GFP::HPH*	This study
BWY6056	*MATα ura3-1 ade2-1 his3-11, 15 leu2-3112 trp1-1 can1-100 ade2::ADE2 ADH1-OsTIR1-9myc::URA3 HisΔ::URA Pan1-AID::G418 Ade8Δ::LEU RVS167-GFP::HPH*	This study
BWY6061	*MATα ura3-1 ade2-1 his3-11 leu2,3112 trp1-1 can1-100 ade2::ADE2 Ade8Δ::LEU Sla1-GFP::HPH Sac6-RFP::G418*	This study
BWY6062	*MATα ura3-1 ade2-1 his3-11, 15 leu2-3112 trp1-1 can1-100 ade2::ADE2 ADH1-OsTIR1-9myc::URA3 HisΔ::URA Ade8Δ::LEU Sla1-GFP::HPH Sac6-RFP::G418*	This study
BWY6063	*MATα ura3-1 ade2-1 his3-11, 15 leu2-3112 trp1-1 can1-100 ade2::ADE2 ADH1-OsTIR1-9myc::URA3 HisΔ::URA Pan1-AID::G418 Ade8Δ::LEU Sla1-GFP::HPH Sac6-RFP::G418*	This study
BWY6111	*MATα ura3-1 ade2-1 his3-11 leu2,3112 trp1-1 can1-100 ade2::ADE2 Ade8Δ::LEU Sla2-GFP::HPH Sac6-RFP::G418*	This study
BWY6112	*MATα ura3-1 ade2-1 his3-11, 15 leu2-3112 trp1-1 can1-100 ade2::ADE2 ADH1-OsTIR1-9myc::URA3 HisΔ::URA Ade8Δ::LEU Sla2-GFP::HPH Sac6-RFP::G418*	This study
BWY6113	*MATα ura3-1 ade2-1 his3-11, 15 leu2-3112 trp1-1 can1-100 ade2::ADE2 ADH1-OsTIR1-9myc::URA3 HisΔ::URA Pan1-AID::G418 Ade8Δ::LEU Sla2-GFP::HPH Sac6-RFP::G418*	This study

TABLE 3: Strains used in this study.

Continues

Strain	Genotype	Source
BWY6071	*MATα ura3-1 ade2-1 his3-11 leu2,3112 trp1-1 can1-100 ade2::ADE2 Ade8Δ::LEU End3-GFP::HPH Sac6-RFP::G418*	This study
BWY6072	*MATα ura3-1 ade2-1 his3-11, 15 leu2-3112 trp1-1 can1-100 ade2::ADE2 ADH1-OsTIR1-9myc::URA3 HisΔ::URA Ade8Δ::LEU End3-GFP::HPH Sac6-RFP::G418*	This study
BWY6073	*MATα ura3-1 ade2-1 his3-11, 15 leu2-3112 trp1-1 can1-100 ade2::ADE2 ADH1-OsTIR1-9myc::URA3 HisΔ::URA Pan1-AID::G418 Ade8Δ::LEU End3-GFP::HPH Sac6-RFP::G418*	This study
BWY6068	*MATα ura3-1 ade2-1 his3-11 leu2,3112 trp1-1 can1-100 ade2::ADE2 Ade8Δ::LEU Ede1-GFP::HPH Sac6-RFP::G418*	This study
BWY6069	*MATα ura3-1 ade2-1 his3-11, 15 leu2-3112 trp1-1 can1-100 ade2::ADE2 ADH1-OsTIR1-9myc::URA3 HisΔ::URA Ade8Δ::LEU Ede1-GFP::HPH Sac6-RFP::G418*	This study
BWY6070	*MATα ura3-1 ade2-1 his3-11, 15 leu2-3112 trp1-1 can1-100 ade2::ADE2 ADH1-OsTIR1-9myc::URA3 HisΔ::URA Pan1-AID::G418 Ade8Δ::LEU Ede1-GFP::HPH Sac6-RFP::G418*	This study
BWY6065	*MATα ura3-1 ade2-1 his3-11 leu2,3112 trp1-1 can1-100 ade2::ADE2 Ade8Δ::LEU Myo5-GFP::HPH Sac6-RFP::G418*	This study
BWY6066	*MATα ura3-1 ade2-1 his3-11, 15 leu2-3112 trp1-1 can1-100 ade2::ADE2 ADH1-OsTIR1-9myc::URA3 HisΔ::URA Ade8Δ::LEU Myo5-GFP::HPH Sac6-RFP::G418*	This study
BWY6067	*MATα ura3-1 ade2-1 his3-11, 15 leu2-3112 trp1-1 can1-100 ade2::ADE2 ADH1-OsTIR1-9myc::URA3 HisΔ::URA Pan1-AID::G418 Ade8Δ::LEU Myo5-GFP::HPH Sac6-RFP::G418*	This study
BWY5969	*MATα ura3-1 ade2-1 his3-11 leu2,3112 trp1-1 can1-100 ade2::ADE2 Ade8Δ::LEU Las17-GFP::G418*	This study
BWY5970	*MATα ura3-1 ade2-1 his3-11, 15 leu2-3112 trp1-1 can1-100 ade2::ADE2 ADH1-OsTIR1-9myc::URA3 HisΔ::URA Ade8Δ::LEU Las17-GFP::G418*	This study
BWY5971	*MATα ura3-1 ade2-1 his3-11, 15 leu2-3112 trp1-1 can1-100 ade2::ADE2 ADH1-OsTIR1-9myc::URA3 HisΔ::URA Pan1-AID::G418 Ade8Δ::LEU Las17-GFP::G418*	This study
BWY6230	*MATα ura3-1 ade2-1 his3-11 leu2,3112 trp1-1 can1-100 ade2::ADE2 Ade8Δ::LEU Sac6-RFP::G418*	This study
BWY6231	*MATα ura3-1 ade2-1 his3-11, 15 leu2-3112 trp1-1 can1-100 ade2::ADE2 ADH1-OsTIR1-9myc::URA3 HisΔ::URA Ade8Δ::LEU Sac6-RFP::G418*	This study
BWY6232	*MATα ura3-1 ade2-1 his3-11, 15 leu2-3112 trp1-1 can1-100 ade2::ADE2 ADH1-OsTIR1-9myc::URA3 HisΔ::URA Pan1-AID::G418 Ade8Δ::LEU Sac6-RFP::G418*	This study

TABLE 3: Strains used in this study. Continued

with 1 μg/ml propidium iodide. Five thousand cells were immediately analyzed on a BD FACSCalibur (Becton Dickinson, Mountain View, CA) flow cytometry system to quantify the population of cells with fluorescent propidium iodide staining.

FM4-64 staining

FM4-64 images were collected using a Zeiss Axiovert 135TV inverted microscope (Carl Zeiss MicroImaging, Thornwood, NY) with a Sensicam QE charge-coupled device (CCD) camera (Cooke, Romulus, MI), Zeiss 100×/1.4 numerical aperture (NA) Plan-Apochromat objective, motorized filter wheels, fluorescein isothiocyanate (FITC) and Texas Red filter sets (Semrock, Rochester, NY), and SlideBook 5.0 software (Intelligent Imaging Innovations, Denver, CO). Images were captured with 500-ms exposure and identical binning, intensification, and illumination intensity. Log-phase cells were incubated in YNB –Trp media minus or plus 500 μM IAA for 30 min at 30°C. For FM4-64 labeling, cell aliquots were transferred to an Eppendorf tube with 10 μg/ml FM4-64 (Molecular Probes, Eugene, OR) and incubated for 15 min at 30°C. The cells were washed twice with fresh medium to remove excess FM4-64, resuspended in 100 μl of fresh medium, and then put on ice until visualization at the microscope. Cells were spotted onto uncoated glass slides and covered with a coverslip.

Fluorescence microscopy

Mup1-pHl. Mup1-pHluorin images were collected using a Zeiss Axiovert 135TV inverted with a Sensicam QE CCD camera, Zeiss 100×/1.4 NA Plan-Apochromat objective, motorized filter wheels, FITC and Texas Red filter sets (Semrock), and SlideBook 5.0 software. Images were captured with 500-ms exposure and identical binning, intensification, and illumination intensity. For quantification of fluorescence intensity, 16-bit image files were analyzed in ImageJ, version 1.41n (National Institutes of Health, Bethesda, MD). Background subtraction was performed before measurement of integrated density, and values were corrected for cell size.

To perform kinetic analysis of endocytosis, cells expressing Mup1-pHluorin were grown overnight in synthetic YNB medium lacking methionine (YNB–Met). Cells were then diluted to a density of 0.35 OD/ml in YNB–Met and grown to a density of 0.6 OD/ml. Cells were then seeded onto concanavalin A–coated eight-well glass-bottomed chamber slides (LabTek, Scotts Valley, CA) containing YNB–Met and allowed to settle before imaging. Cells were or were not treated with 500 μM IAA for 30 min, and then methionine was added at a concentration of 20 μg/ml, and images were captured after 30 min or 1 h. During image acquisition, cells were maintained at a constant temperature of 30°C. Experiments with Pan1 plasmids were performed in YNB–Trp–Met medium.

Plasmid	Details	Description	Source
pRS414	*CEN, TRP1*		Laboratory plasmid
pBW373	pRS426::GFP-PH of PLC(delta)	GFP-PH (*2μ, URA3*)	Emr lab
pBW626	pRS414::*PAN1 (CEN, TRP1)*	pPan1.414	Sachs *et al*. (1992)
pBW628	pRS414::*pan1*(AA1-97, 390-1480) *(CEN, TRP1)*	pPan1 AA: 1-97, 390-1480.414	Sachs *et al*. (1992)
pBW630	pRS414::*pan1*(AA1-855) *(CEN, TRP1)*	pPan1 AA: 1-855.414	Sachs *et al*. (1992)
pBW1443	pRS414::*PAN1-GFP (CEN, TRP1)*	pPan1-GFP.414	Laboratory plasmid
pBW2508	pRS414::*pan1*(AA250-855) *(CEN, TRP1)*	pPan1 AA: 250-855.414	This study
pBW2581	pRS414::*pan1*(AA1-702)-GFP *(CEN, TRP1)*	pPan1 AA: 1-702-GFP.414	This study
pBW2582	pRS414::*pan1*(AA1-1050)-GFP *(CEN, TRP1)*	pPan1 AA: 1-1050-GFP.414	This study
pBW2583	pRS414::*pan1*(AA702-1480)-GFP *(CEN, TRP1)*	pPan1 AA: 702-1480-GFP.414	This study
pBW2584	pRS414::*pan1*(AA1050-1480)-GFP *(CEN, TRP1)*	pPan1 AA:1050-1480-GFP.414	This study
pBW2594	pRS414::*pan1*(AA702-1050)-GFP *(CEN, TRP1)*	pPan1 AA: 702-1050-GFP.414	This study
pBW2597	pRS414::*pan1*(AA1-97,402-855) *(CEN, TRP1)*	pPan1 AA: 1-97, 402-855.414	This study
pBW2623	pRS414::*pan1*(AA402-1050)-GFP *(CEN, TRP1)*	pPan1 AA: 402-1050-GFP.414	This study
pBW2624	pRS414::*pan1*(AA1-855)-GFP *(CEN, TRP1)*	pPan1 AA: 1-855-GFP.414	This study
pBW2626	pRS414::*pan1*(AA402-855)-GFP *(CEN, TRP1)*	pPan1 AA: 402-855-GFP.414	This study
pBW2627	pRS414::*pan1*(AA1-97, 402-855)-GFP *(CEN, TRP1)*	pPan1 AA: 1-97, 402-855-GFP.414	This study
pBW2642	pRS414::*pan1*(AA1-390, 680-1480) *(CEN, TRP1)*	pPan1 AA: 1-390, 680-1480.414	This study
pBW2645	pRS414::*pan1*(AA402-855) *(CEN, TRP1)*	pPan1 AA: 402-855.414	This study
pBW2696	pRS414::*pan1*(AA1-401, 856-1480 *(CEN, TRP1)*	pPan1 AA: 1-401, 856-1480.414	This study
pBW2723	pRS414::*pan1*(AA402-1050) *(CEN, TRP1)*	pPan1 AA: 402-1050.414	This study
pBW2780	pRS414::*pan1*(AA402-1480) *(CEN, TRP1)*	pPan1 AA: 402-1480.414	This study
pBW2789	pRS414::*pan1*(AA1-97, 680-1480) *(CEN, TRP1)*	pPan1 AA: 1-97, 680-1480.414	This study
pBW2795	pRS414::*pan1*(AA1-702) *(CEN, TRP1)*	pPan1 AA: 1-702.414	This study
pBW2797	pRS414::*pan1*(AA250-855)-GFP *(CEN, TRP1)*	pPan1 AA:250-855-GFP.414	This study
pBW2841	pRS414::*pan1*(AA1-401, 856-1480)-GFP *(CEN, TRP1)*	pPan1 AA:1-401, 856-1480-GFP.414	This study

TABLE 4: Plasmids used in this study.

GFP/RFP time-lapse collections. Log-phase cells were incubated with or without 500 μM IAA for 45 min to 1 h at 30°C and then imaged using the Zeiss AxioObserver Yokogawa CSU-X1 spinning disk confocal. Movies were captured with 150- to 200-ms exposure at 0.5–4 s/frame for 90–120 frames. Lifetimes of >50 individual patches for each strain were recorded and averaged together using ImageJ. Patch number per micrometer of cell perimeter was counted for >30 cells/strain and averaged using ImageJ. Representative kymographs were generated with Zen software.

Image/statistical analysis

Statistical significance between populations was determined by one-way analysis of variance followed by Tukey's multiple comparison post hoc analysis.

ACKNOWLEDGMENTS

We thank the members of the Wendland laboratory for helpful discussion and sharing of ideas and reagents, especially Alex Wade, Kristie Wrasman, and Daniel Pierce for their help in plasmid construction and critiques of the manuscript. We thank Nathan Wright and Johanna Poprowski for technical assistance. We thank Michael McCaffery and Erin Pryce of the Integrated Imaging Center for help with light microscopy. We thank the Nishimura, Drubin, Riezman, Pruyne, Hicke, and Sachs labs for plasmids and antibodies. Finally, we thank Chris Stefan and Adam Kim of the Cunningham lab for help with flow cytometry experiments. This work was funded by Grant RO1 GM60979 from the National Institutes of Health (NIH) to B.W. M.K.B. and K.W. were in part supported by an NIH T32 Training Grant (T32 007231-37).

REFERENCES

Barker SL, Lee L, Pierce BD, Maldonado-Baez L, Drubin DG, Wendland B (2007). Interaction of the endocytic scaffold protein Pan1 with the type I myosins contributes to the late stages of endocytosis. Mol Biol Cell 18, 2893–2903.

Bidlingmaier S, Weiss EL, Seidel C, Drubin DG, Snyder M (2001). The Cbk1p pathway is important for polarized cell growth and cell separation in Saccharomyces cerevisiae. Mol Cell Biol 21, 2449–2462.

Boeke D, Trautmann S, Meurer M, Wachsmuth M, Godlee C, Knop M, Kaksonen M (2014). Quantification of cytosolic interactions identifies Ede1 oligomers as key organizers of endocytosis. Mol Syst Biol 10, 756.

Chu DS, Pishvaee B, Payne GS (1996). The light chain subunit is required for clathrin function in Saccharomyces cerevisiae. J Biol Chem 271, 33123–33130.

Duncan MC, Cope MJ, Goode BL, Wendland B, Drubin DG (2001). Yeast Eps15-like endocytic protein, Pan1p, activates the Arp2/3 complex. Nat Cell Biol 3, 687–690.

Gagny B, Wiederkehr A, Dumoulin P, Winsor B, Riezman H, Haguenauer-Tsapis R (2000). A novel EH domain protein of Saccharomyces cerevisiae, Ede1p, involved in endocytosis. J Cell Sci 113, 3309–3319.

Goldstein AL, McCusker JH (1999). Three new dominant drug resistance cassettes for gene disruption in Saccharomyces cerevisiae. Yeast 15, 1541–1553.
Hussain NK, Yamabhai M, Ramjaun AR, Guy AM, Baranes D, O'Bryan JP, Der CJ, Kay BK, McPherson PS (1999). Splice variants of intersectin are components of the endocytic machinery in neurons and nonneuronal cells. J Biol Chem 274, 15671–15677.
Kaksonen M, Sun Y, Drubin DG (2003). A pathway for association of receptors, adaptors, and actin during endocytic internalization. Cell 115, 475–487.
Kaksonen M, Toret CP, Drubin DG (2005). A modular design for the clathrin- and actin-mediated endocytosis machinery. Cell 123, 305–320.
Kamińska J, Sedek M, Wysocka-Kapcińska M, Zoładek T (2007). Characterization of nuclear localization and nuclear export signals of yeast actin-binding protein Pan1. FEBS Lett 581, 5371–5376.
Kamińska J, Wysocka-Kapcińska M, Smaczyńska-de Rooij I, Rytka J, Zoładek T (2005). Pan1p, an actin cytoskeleton-associated protein, is required for growth of yeast on oleate medium. Exp Cell Res 310, 482–492.
Longtine MS, McKenzie A, Demarini DJ, Shah NG, Wach A, Brachat A, Philippsen P, Pringle JR (1998). Additional modules for versatile and economical PCR-based gene deletion and modification in Saccharomyces cerevisiae. Yeast 14, 953–961.
Madania A, Dumoulin P, Grava S, Kitamoto H, Schärer-Brodbeck C, Soulard A, Moreau V, Winsor B (1999). The Saccharomyces cerevisiae homologue of human Wiskott-Aldrich syndrome protein Las17p interacts with the Arp2/3 complex. Mol Biol Cell 10, 3521–3538.
Maldonado-Baez L, Dores MR, Perkins EM, Drivas TG, Hicke L, Wendland B (2008). Interaction between Epsin/Yap180 adaptors and the scaffolds Ede1/Pan1 is required for endocytosis. Mol Biol Cell 19, 2936–2948.
Miesenböck G, De Angelis DA, Rothman JE (1998). Visualizing secretion and synaptic transmission with pH-sensitive green fluorescent proteins. Nature 394, 192–195.
Miliaras NB, Wendland B (2004). EH proteins: multivalent regulators of endocytosis (and other pathways). Cell Biochem Biophys 41, 295–318.
Newpher TM, Lemmon SK (2006). Clathrin is important for normal actin dynamics and progression of Sla2p-containing patches during endocytosis in yeast. Traffic 7, 574–588.
Nishimura K, Fukagawa T, Takisawa H, Kakimoto T, Kanemaki M (2009). An auxin-based degron system for the rapid depletion of proteins in nonplant cells. Nat Methods 6, 917–922.
Paoluzi S, Castagnoli L, Lauro I, Salcini AE, Coda L, Fre S, Confalonieri S, Pelicci PG, Di Fiore PP, Cesareni G (1998). Recognition specificity of individual EH domains of mammals and yeast. EMBO J 17, 6541–6550.
Payne GS, Baker D, van Tuinen E, Schekman R (1988). Protein transport to the vacuole and receptor-mediated endocytosis by clathrin heavy chain-deficient yeast. J Cell Biol 106, 1453–1461.
Pierce BD, Toptygin D, Wendland B (2013). Pan1 is an intrinsically disordered protein with homotypic interactions. Proteins 81, 1944–1963.
Prosser DC, Drivas TG, Maldonado-Baez L, Wendland B (2011). Existence of a novel clathrin-independent endocytic pathway in yeast that depends on Rho1 and formin. J Cell Biol 195, 657–671.
Prosser DC, Whitworth K, Wendland B (2010). Quantitative analysis of endocytosis with cytoplasmic pHluorin chimeras. Traffic 11, 1141–1150.
Prusty R, Grisafi P, Fink GR (2004). The plant hormone indoleacetic acid induces invasive growth in Saccharomyces cerevisiae. Proc Natl Acad Sci USA 101, 4153–4157.
Sachs AB, Deardorff JA (1992). Translation initiation requires the PAB-dependent poly(A) ribonuclease in yeast. Cell 70, 961–973.
Salcini AE, Confalonieri S, Doria M, Santolini E, Tassi E, Minenkova O, Cesareni G, Pelicci PG, Di Fiore PP (1997). Binding specificity and in vivo targets of the EH domain, a novel protein-protein interaction module. Genes Dev 11, 2239–2249.
Sengar AS, Wang W, Bishay J, Cohen S, Egan SE (1999). The EH and SH3 domain Ese proteins regulate endocytosis by linking to dynamin and Eps15. EMBO J 18, 1159–1171.
Skruzny M, Brach T, Ciuffa R, Rybina S, Wachsmuth M, Kaksonen M (2012). Molecular basis for coupling the plasma membrane to the actin cytoskeleton during clathrin-mediated endocytosis. Proc Natl Acad Sci USA 109, E2533–E2542.
Stefan CJ, Audhya A, Emr SD (2002). The yeast synaptojanin-like proteins control the cellular distribution of phosphatidylinositol (4,5)-bisphosphate. Mol Biol Cell 13, 542–557.
Stimpson HEM, Toret CP, Cheng AT, Pauly BS, Drubin DG (2009). Early-arriving Syp1p and Ede1p function in endocytic site placement and formation in budding yeast. Mol Biol Cell 20, 4640–4651.
Suzuki R, Toshima JY, Toshima J (2012). Regulation of clathrin coat assembly by Eps15 homology domain-mediated interactions during endocytosis. Mol Biol Cell 23, 687–700.
Tang HY, Cai M (1996). The EH-domain-containing protein Pan1 is required for normal organization of the actin cytoskeleton in Saccharomyces cerevisiae. Mol Cell Biol 16, 4897–4914.
Tang HY, Munn A, Cai M (1997). EH domain proteins Pan1p and End3p are components of a complex that plays a dual role in organization of the cortical actin cytoskeleton and endocytosis in Saccharomyces cerevisiae. Mol Cell Biol 17, 4294–4304.
Tang HY, Xu J, Cai M (2000). Pan1p, End3p, and S1a1p, three yeast proteins required for normal cortical actin cytoskeleton organization, associate with each other and play essential roles in cell wall morphogenesis. Mol Cell Biol 20, 12–25.
Toshima J, Toshima JY, Duncan MC, Cope MJTV, Sun Y, Martin AC, Anderson S, Yates JR, Mizuno K, Drubin DG (2007). Negative regulation of yeast Eps15-like Arp2/3 complex activator, Pan1p, by the Hip1R-related protein, Sla2p, during endocytosis. Mol Biol Cell 18, 658–668.
Toshima J, Toshima JY, Martin AC, Drubin DG (2005). Phosphoregulation of Arp2/3-dependent actin assembly during receptor-mediated endocytosis. Nat Cell Biol 7, 246–254.
Wendland B, Emr SD (1998). Pan1p, yeast eps15, functions as a multivalent adaptor that coordinates protein-protein interactions essential for endocytosis. J Cell Biol 141, 71–84.
Wendland B, McCaffery JM, Xiao Q, Emr SD (1996). A novel fluorescence-activated cell sorter-based screen for yeast endocytosis mutants identifies a yeast homologue of mammalian eps15. J Cell Biol 135, 1485–1500.
Wendland B, Steece KE, Emr SD (1999). Yeast epsins contain an essential N-terminal ENTH domain, bind clathrin and are required for endocytosis. EMBO J 18, 4383–4393.
Whitworth K, Bradford MK, Camara N, Wendland B (2014). Targeted disruption of an EH-domain protein endocytic complex, Pan1-End3. Traffic 15, 43–59.
Wong KA, Wilson J, Russo A, Wang L, Okur MN, Wang X, Martin NP, Scappini E, Carnegie GK, O'Bryan JP (2012). Intersectin (ITSN) family of scaffolds function as molecular hubs in protein interaction networks. PLoS One 7, e36023.
Yamabhai M, Hoffman NG, Hardison NL, McPherson PS, Castagnoli L, Cesareni G, Kay BK (1998). Intersectin, a novel adaptor protein with two Eps15 homology and five Src homology 3 domains. J Biol Chem 273, 31401–31407.
Zeng G, Huang B, Neo SP, Wang J, Cai M (2007). Scd5p mediates phosphoregulation of actin and endocytosis by the type 1 phosphatase Glc7p in yeast. Mol Biol Cell 18, 4885–4898.
Zeng G, Yu X, Cai M (2001). Regulation of yeast actin cytoskeleton-regulatory complex Pan1p/Sla1p/End3p by serine/threonine kinase Prk1p. Mol Biol Cell 12, 3759–3772.
Zoladek T, Vaduva G, Hunter LA, Boguta M, Go BD, Martin NC, Hopper AK (1995). Mutations altering the mitochondrial-cytoplasmic distribution of Mod5p implicate the actin cytoskeleton and mRNA 3′ ends and/or protein synthesis in mitochondrial delivery. Mol Cell Biol 15, 6884–6894.